Theoret. Chim. Acta (Berl.) 34, 277—292 (1974)

Conformation of Ethylene Glycol*: Isometric Group, *ab initio* Study of Internal H Bonding and IR-Matrix Spectra of the Species CH_2OHCH_2OH, CD_2OHCD_2OH and CH_2ODCH_2OD

Tae-Kyu Ha, H. Frei, R. Meyer, and Hs. H. Günthard

Laboratory of Physical Chemistry, Swiss Federal Institute of Technology, Zürich, Switzerland

Received January 22, 1974

The isometric group of a semirigid model of the ethylene glycol molecule with 3 internal degrees of freedom is derived. Results of extensive *ab initio* computation of the electronic potential function with a Gaussian lobe basis set are presented from which two different r_e conformations are predicted. Both feature one single internal H bond in which one of the lone electron pairs of the acceptor O atom is involved. Symmetry sets of isometric r_e-conformations and of transition points of the potential function are discussed. Infrared matrix spectra of glycol and 2 deuterated modifications are presented and discussed on the basis of two internally bonded conformations predicted by *ab initio* calculations.

Key words: Ethylene glycol, conformation of ~ – bonding – Isometric group of glycol

1. Introduction

Structural investigation of monomeric ethylene glycol is of interest with respect to nonlinear hydrogen bonding and as a structural constituent of many biological molecules. There exists a considerable body of experimental data on glycol dissolved in a variety of solvents. Many of these relate to systems with pronounced tendency to formation of H bonds between solvent and dissolved glycol molecules. For recent NMR study including extended citations of literature the reader is referred to Pachler [1]. Similarly an infrared and Raman study of liquid glycol has been reported by Matsura *et al.* [2]. It should be pointed out that discussion of the conformations of the glycol molecule based on such data remain questionable.

Experimental studies on the free molecule include the electron diffraction work by Bastiansen [4] and also the gas-phase infrared studies by Buckley [5] and Zubkova *et al.* [6, 7]. They concluded that only the gauche conformation with respect to the C–C bond involving a single internal hydrogen bond is present in ethylene glycol. However, no experimental information seems to be available on the OH conformations. More detailed conformational studies were reported on related molecules such as haloethanols [8, 9] and aminoethanol [10].

* Dedicated to Prof. H. Hartmann on the occasion of his 60th birthday.

There have been reported two theoretical studies on the conformation problem of the free glycol molecule. Radom *et al.* [3] reported a study of the conformational problem of ethylene glycol by LCAO SCF molecular orbital calculations in the 1,2-disubstituted ethanes series. As a basis set Pople's 4-31 *G* basis [23] was used to calculate the electronic potential of 6 gauche conformations (cf. Table 5). According to this paper the *tGg'* conformation is predicted to represent the lowest energy nuclear configuration and no other stable low energy conformations have been found. The *tGg'* conformer (corresponding to the nuclear configuration $2\tau = 60°$, $\upsilon_0 = -60°$, $\upsilon_1 = 180°$ in our notation, cf. Fig. 1b) features one internal hydrogen bond. The *tTt* conformation ($2\tau = 180°$, $\upsilon_0 = \upsilon_1 = 180°$) was predicted to possess only 2.01 kcal/mol higher energy than the stable *tGg'* form. This finding is rather surprising in view of the small line width observed for the internally bonded OH-stretching band [11] indicating low anharmonicity and nearly no predissociation.

A theoretical analysis of intramolecular interactions has recently been published by Podo *et al.* [12] based on a Scott-Scheraga type model [13]. Among the results of this work the *tGg'* conformer again was found to be the most stable one. However, the most stable trans conformation *gTg'* ($2\tau = 180°$, $\upsilon_0 = -\upsilon_1 = \pm 60°$) was obtained to have 1.27 kcal/mol higher energy than *tGg'*, in contrast to Pople's results.

In the present work a further contribution to the glycol conformation problem is reported. It includes a study of the internal isometric group [14] for a model involving three internal rotational degrees of freedom (Section 2), an *ab initio* quantum chemical calculation (Section 3) and a discussion of parts of new infrared spectra of 3 matrix-isolated isotopic ethylene glycol species in particular with regard to conformational effects (Section 4). *Ab initio* calculations were carried out with a Whitten type Gaussian lobe extended basis set for 25 gauche conformations ($2\tau = 60°$, $-180° \leqq \upsilon_0$, $\upsilon_1 < 180°$), i.e. for a sufficiently narrowly spaced lattice of the internal rotation angles υ_0, υ_1 to permit reliable interpolation and search for local minima of the potential energy surface (cf. Fig. 2). Two such local minima r_{e1}, r_{e2} respectively, have been found at $\upsilon_0 \approx -30°$, $\upsilon_1 \approx 60°$, and $\upsilon_0 \approx -45°$, $\upsilon_1 \approx -160°$. The former conformation represents the most stable r_e structure. It has not been calculated by Radom *et al.* [3] and therefore has been overlooked. The latter corresponds approximately to the *tGg'* conformer predicted in Radom's work but lies 1.82 kcal/mol higher in energy than r_{e1}. The *tTt* conformer was found to lie 7.03 kcal/mol higher than the $2\tau = 60°$, $\upsilon_0 = -30°$, $\upsilon_1 = 60°$ conformation (r_{e1} structure), in sharp contrast to Radom's result. As a whole the present calculation yielded electronic energies which are approximately 0.1 a.u. lower than those found by Radom for corresponding conformations, cf. Table 5.

The results of the *ab initio* calculations are then correlated with the matrix spectra of 3 isotopic species of glycol. The spectra may be interpreted in close agreement with the predicted potential energy surface. Knudsen cell experiments carried out at 160° C cell temperature yielded matrix spectra essentially identical with those obtained at room temperature. This fact is compatible with the findings that the *tTt* conformation has 7 kcal/mol higher energy than the r_{e1} structure.

2. Isometric Group of Glycol

In this section the isometric group of a molecular model of the glycol molecule with 3 internal degrees of freedom will be discussed. The manifold of conformations of this molecule may be described by the dihedral angle 2τ of the internal rotation around the C–C bond ($\tau = 0$ for cis-conformation) and by the two dihedral angles υ_0, υ_1 of the two OH internal rotations ($\upsilon_0 = \upsilon_1 = 0$ for the respective cis conformations). A schematic drawing of the model is given in Figs. 1a, b. Besides the three finite degrees of freedom no further internal degrees of freedom will be considered.

The isometric group, i.e. the symmetry group of the nonrigid glycol model is determined by the group of substitutions $\mathscr{F}\{\tau, \upsilon_0, \upsilon_1\}$, which maps the graph $\mathscr{N}\{P(\Pi_k(Z_k, M_k)), K(d_{kk'})\}$ associated with the nuclear configuration onto itself [14]

$$\begin{pmatrix} \tau' \\ \upsilon_0' \\ \upsilon_1' \\ 1 \end{pmatrix} = \begin{pmatrix} A(F) & a(F) \\ 0 & 1 \end{pmatrix} \begin{pmatrix} \tau \\ \upsilon_0 \\ \upsilon_1 \\ 1 \end{pmatrix}. \tag{2-1}$$

For derivation of this group the coordinate vectors of sets of equivalent nuclei given in Table 1 may be used. These describe both the points of the frame and of the two tops. For the sake of generality, a set of 4 equivalent nuclei of the

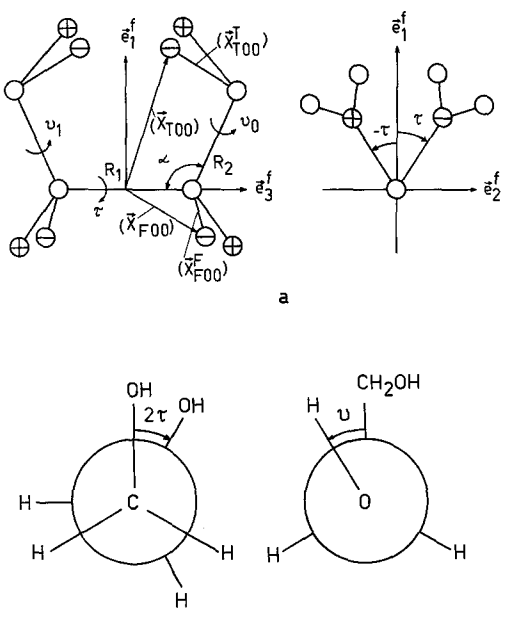

b

Fig. 1a and b. Semirigid model of ethylene glycol. a Schematics of molecular structural parameters and coordinate systems. b Newman projections for definition of internal rotational degrees of freedom

Table 1. Coordinate vectors of equivalent nuclei of semirigid ethylene glycol molecule

Set	Vector[a]	X
frame $\lambda, \varkappa = 0, 1$	$X_{F\lambda\varkappa}$	$\begin{pmatrix} 1 & & \\ & -1 & \\ & & -1 \end{pmatrix}^{\lambda} \left\{ \frac{1}{2} R_1 \cdot \begin{pmatrix} 0 \\ 0 \\ 1 \end{pmatrix} + \begin{pmatrix} c\tau & -s\tau & 0 \\ s\tau & c\tau & 0 \\ 0 & 0 & 1 \end{pmatrix} \cdot \begin{pmatrix} 1 & & \\ & (-1)^{\varkappa} & \\ & & 1 \end{pmatrix} X^{F}_{F00}{}^{b} \right\}$
top λ $\lambda, \varkappa = 0, 1$	$X_{T\lambda\varkappa}$	$\begin{pmatrix} 1 & & \\ & -1 & \\ & & -1 \end{pmatrix}^{\lambda} \left\{ \frac{1}{2} R_1 \cdot \begin{pmatrix} 0 \\ 0 \\ 1 \end{pmatrix} + \begin{pmatrix} c\tau & -s\tau & 0 \\ s\tau & c\tau & 0 \\ 0 & 0 & 1 \end{pmatrix} \cdot \begin{pmatrix} c\alpha & 0 & s\alpha \\ 0 & 1 & 0 \\ -s\alpha & 0 & c\alpha \end{pmatrix} \left[R_2 \cdot \begin{pmatrix} 0 \\ 0 \\ 1 \end{pmatrix} + \begin{pmatrix} c\upsilon_{\lambda} & -s\upsilon_{\lambda} & 0 \\ s\upsilon_{\lambda} & c\upsilon_{\lambda} & 0 \\ 0 & 0 & 1 \end{pmatrix} \cdot \begin{pmatrix} 1 & & \\ & (-1)^{\varkappa} & \\ & & 1 \end{pmatrix} X^{T}_{T00}{}^{b} \right] \right\}$

[a] Coordinates refer to the coordinate system $\tilde{e}^{f}$ indicated in Fig. 1; similarly the structural parameters R_1, R_2, α are defined in Fig. 1, where α corresponds to $\pi-\alpha$ of Fig. 1.

[b] Coordinate vector of representative nucleus w.r.t. local coordinate system $\tilde{e}^{F}$ resp. $\tilde{e}^{T}$.

frame (representative coordinate vector X_{F00}) and a set of 2 equivalent nuclei for each of the two tops with local symmetry C_s (representative coordinate vectors X_{T00}, X_{T10}) are chosen.

From the coordinate vectors given in Table 1 one obtains through the elementary relation

$$d^2_{kk'} = \widetilde{(X_k - X_{k'})}(X_k - X_{k'})$$

sets of distances expressed as functions of the internal rotation angles τ, υ_0, υ_1. Study of the substitutions of type (2-1) which map such sets of distances onto themselves yields the group $\mathscr{F}(\tau, \upsilon_0, \upsilon_1)$ collected in Table 2. Application of these to the coordinate vectors yields the representation $\Gamma^{(\mathrm{NC})}\{\mathscr{F}\}$ according to

$$\hat{P}_F\{\tilde{X}_{F\lambda\varkappa}(\tau)\} = \{\tilde{X}_{F\lambda\varkappa}(\tau)\}\, \Gamma^{(\mathrm{NCF})}(F)$$

$$\hat{P}_F\{\tilde{X}_{T\lambda\varkappa}(\tau, \upsilon_0, \upsilon_1)\} = \{\tilde{X}_{T\lambda\varkappa}(\tau, \upsilon_0, \upsilon_1)\}\, \Gamma^{(\mathrm{NCT})}(F)$$

which together with the permutation representation $\Gamma^{(\mathscr{N}\mathscr{C})}(\mathscr{F})$ and the substitution group $\Gamma\{\mathscr{F}\}$ of all dynamical variables are listed in Table 2.

Since the covering group $\mathscr{G}(\tau, \upsilon_0, \upsilon_1)$ of nuclear configurations with arbitrary values of the internal coordinates $\tau, \upsilon_0, \upsilon_1$ consists of the identity only, the full isometric group $\mathscr{H} = \mathscr{F}(\tau, \upsilon_0, \upsilon_1) = \mathscr{V}_4$.

The following remarks should be made concerning the isometric group $\mathscr{H}$ of semirigid ethylene glycol:

1. The isometric group given in Table 2 is characteristic for any system with a semirigid frame of symmetry C_2 and two equivalent internal tops of local symmetry C_s. $OHCH_2CH_2OH$ and CH_2F $CH_2CH_2CH_2F$ may be taken as typical molecules. From this group a large number of symmetry groups of further nonrigid molecules may be derived, i.e.
   - $C_{2v}(C_{2h})$ frame with two equivalent tops of local symmetry C_s, like 1,2-dihydroxy benzene (*trans*-1,4-dichlorobutene-2), by freezing τ at 0

Table 2. Internal isometric group of semirigid ethylene glycol type molecules

Operator $F \in \mathscr{F}$	Substitution[a] Group $\Gamma\{\mathscr{F}\}$	Representation[b] $\Gamma^{(\mathrm{NC})}\{\mathscr{F}\}$ $\Gamma^{(\mathrm{NCF})}\{\tilde{X}_{F\lambda\varkappa}(\tau)\}$	$\Gamma^{(\mathrm{NCT})}\{\tilde{X}_{T\lambda\varkappa}(\tau, \upsilon_i)\}$	Representation $\Gamma^{(\mathscr{N}\mathscr{C})}\{\mathscr{F}\}$ $\{d_{T\lambda\varkappa, T\bar{\lambda}\bar{\varkappa}}(\tau, \upsilon_0, \upsilon_1)\}$
E	$\begin{pmatrix} 1 & & & & & & \\ & 1 & & & & & \\ & & 1 & & & & \\ & & & 1 & & & \\ & & & & 1 & & \\ & & & & & 1 & \\ & & & & & & 1 \end{pmatrix}$	$(\delta_{\bar{\lambda}\lambda}\delta_{\bar{\varkappa}\varkappa})\otimes I$	$(\delta_{\bar{\lambda}\lambda}\delta_{\bar{\varkappa}\varkappa})\otimes I$	$\begin{pmatrix} 1 & & & \\ & 1 & & \\ & & 1 & \\ & & & 1 \end{pmatrix}$
V_2	$\begin{pmatrix} 1 & \cdots & \cdots & \pi \\ -1 & \cdots & \cdots & \pi \\ & -1 & \cdots & 0 \\ & & 1 \cdots & 0 \\ & & \cdot\cdot & 10 \\ & & \cdot 1 & \cdot 0 \\ & & & 1 \end{pmatrix}$	$(\delta_{\bar{\lambda}\lambda}\delta_{\bar{\varkappa}\varkappa})\otimes D(e_1^f, \pi)$	$(\delta_{\bar{\lambda}, \lambda+1}\delta_{\bar{\varkappa}\varkappa})\otimes D(e_1^f, \pi)$	$\begin{pmatrix} 1 & \cdots & \cdots \\ \cdots & 1 & \cdot\cdot \\ \cdot\cdot & 1 & \cdots \\ \cdots & \cdots & 1 \end{pmatrix}$
V_3	$\begin{pmatrix} 1 & \cdots & \cdots & \cdots & \pi \\ -1 & \cdots & \cdots & \cdots & \pi \\ & -1 & \cdots & \cdots & \pi \\ & & -1 & \cdots & 0 \\ & & & -1 \cdots & 0 \\ & & & & -10 \\ & & & & 1 \end{pmatrix}$	$(\delta_{\bar{\lambda},\lambda}\delta_{\bar{\varkappa},\varkappa+1})\otimes D(e_2^f, \pi)\cdot Z$	$(\delta_{\bar{\lambda},\lambda}\delta_{\bar{\varkappa},\varkappa+1})\otimes D(e_2^f, \pi) Z$	$\begin{pmatrix} \cdots & \cdots & 1 \\ \cdots & 1 & \cdot\cdot \\ \cdot\cdot & 1 & \cdots \\ 1 & \cdots & \cdots \end{pmatrix}$
V_4	$\begin{pmatrix} 1 & \cdots & \cdots & \cdots & 0 \\ & 1 & \cdots & \cdots & 0 \\ & & 1 & \cdots & \pi \\ & & & -1 \cdots & 0 \\ & & & \cdot & -10 \\ & & & & -1 \cdot 0 \\ & & & & 1 \end{pmatrix}$	$(\delta_{\bar{\lambda},\lambda}\delta_{\bar{\varkappa},\varkappa+1})\otimes D(e_3^f, \pi)\cdot Z$	$(\delta_{\bar{\lambda},\lambda+1}\delta_{\bar{\varkappa},\varkappa+1})\otimes D(e_3^f, \pi) Z$	$\begin{pmatrix} \cdots & \cdots & 1 \\ \cdot\cdot & 1 & \cdots \\ \cdots & 1 & \cdot\cdot \\ 1 & \cdots & \cdots \end{pmatrix}$

[a] Representation of $\mathscr{F}$ by substitutions of the Eulerian angles α, β, γ and the internal coordinates τ, υ_0, υ_1.

[b] $\Gamma^{(\mathrm{NCF})}$: representation generated by the vectors $\tilde{X}_{F00}(\tau)$, $\tilde{X}_{F01}(\tau)$, $\tilde{X}_{F10}(\tau)$, $\tilde{X}_{F11}(\tau)$ of a set of equivalent nuclei in general site of the frame (see Fig. 1). $\Gamma^{(\mathrm{NCT})}$: representation generated by the vectors $\tilde{X}_{T00}(\tau, \upsilon_0)$, $\tilde{X}_{T01}(\tau, \upsilon_0)$, $\tilde{X}_{T10}(\tau, \upsilon_1)$, $\tilde{X}_{T11}(\tau, \upsilon_1)$ of a set of equivalent nuclei in the general site originating from the two equivalent tops of C_s local symmetry (see Fig. 1). I denotes a 3×3 unit matrix. The matrix $D(e, \Phi)$ represents the rotation around axis e through angle Φ and $Z = -I$ represents the center of symmetry. $\Gamma^{(\mathscr{N}\mathscr{C})}$: is the representation by permutations generated by the set of distances $d_{T00,T10}(\tau, \upsilon_0, \upsilon_1)$, $d_{T00,T11}(\tau, \upsilon_0, \upsilon_1)$, $d_{T01,T10}(\tau, \upsilon_0, \upsilon_1)$, $d_{T01,T11}(\tau, \upsilon_0, \upsilon_1)$ originating from the two equivalent tops of C_s local symmetry (see Fig. 1).

- C_s frame, C_s top system by freezing τ, υ_0 at 0 or π, like CH_2DOH,
- two equivalent C_s top system, by freezing υ_0, υ_1 at 0, π; a typical representative for this system is the glyoxal molecule.

2. The internal isometric group may be used to reduce the number of points of the electronic energy function $\mathscr{E}(\tau, \upsilon_0, \upsilon_1)$ to be calculated, by the fact that all isometric nuclear configurations have equal electronic energy. This will show up in the *ab initio* calculations presented in Section 3 and reflects itself in the symmetry of the electronic energy function: for any operator $\hat{P}_F$ associated

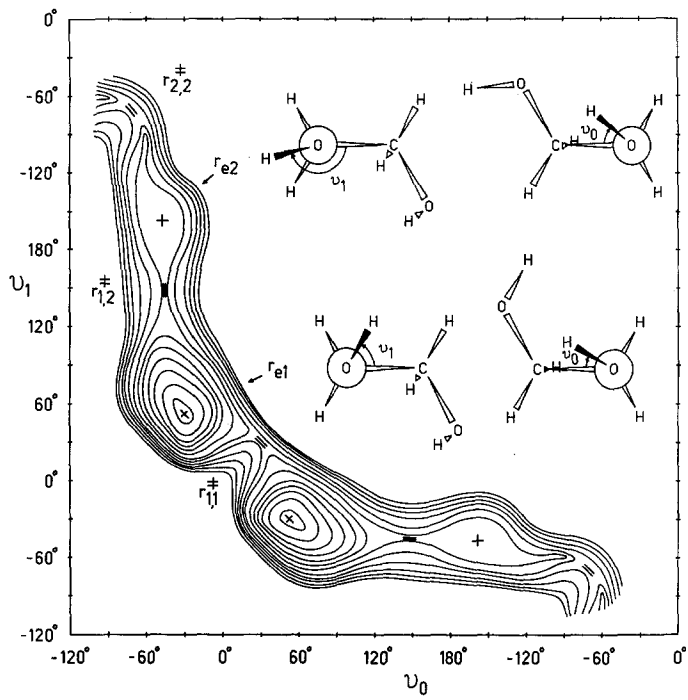

Fig. 2. Section of the Born-Oppenheimer energy surface. Electronic energy diagram from the *ab initio* SCF calculation of $\mathscr{E}(\upsilon_0, \upsilon_1)$ for $2\tau = 60°$. The upper two models correspond to the r_{e2}-conformer and the lower two models correspond to the r_{e1}-conformers. The energy levels are separated by 5×10^{-4} a.u. (110 cm^{-1})

with the substitutions (2-1) we have

$$\hat{P}_F \mathscr{E}(\tau, \upsilon_0, \upsilon_1) = \mathscr{E}(\tau, \upsilon_0, \upsilon_1) \tag{2-2}$$

3. The internal isometric group may likewise be used to derive domains of uniqueness for the continuum of nuclear configurations defined by the 3 internal coordinates. In this paper the following choice will be made

$$\begin{aligned} -\frac{\pi}{2} < \tau \leqq +\frac{\pi}{2} \\ -\pi < \upsilon_0, \upsilon_1 \leqq +\pi\,. \end{aligned} \tag{2-3}$$

4. As a consequence of (2-2), to any r_e structure with a local minimum of the electronic energy function occuring in the interval (2-3), say at τ_e, υ_{0e}, υ_{1e} there must exist 3 further isometric NC with the same value of the electronic energy, namely those with coordinates (cf. Table 2)

$$\begin{array}{lll} \tau_e\,, & \upsilon_{1e}\,, & \upsilon_{0e} \\ -\tau_e\,, & -\upsilon_{0e}\,, & -\upsilon_{1e} \\ -\tau_e\,, & -\upsilon_{1e}\,, & -\upsilon_{0e}\,. \end{array}$$

There may occur several non-isometric r_e structures within the domain (2-3), as is indeed the case for ethylene glycol, cf. Section 3, Fig. 2.

It should be pointed out that such r_e structures do not correspond to nuclear motion energy eigenstates of the Hamiltonian. Nevertheless, they may be prepared experimentally by means of external fields (e.g. chemical reactions) if the spontaneous relaxation to energy eigenstates is slow enough. Under this condition, in the case at hand, the non-isometric r_e structures represent different conformations of the glycol molecule, which may be observed by appropriate experimental methods (see Section 4).

In general, however, the molecular eigenstates belong to irreducible representations of the isometric group and therefore study of these states does not allow identification of particular conformations.

5. The permutation parts in the representations $\Gamma^{(NC)}$ given in Table 2 represent the Longuet-Higgins group of the semirigid model. Since for a set of equivalent points of the frame the operator V_2 is represented either by a mapping alone or a permutation alone, the representation $\Gamma^{(NCF)}\{\mathscr{F}\}$ may be chosen in two isomorphic forms; however, only one of these is given.
6. The representation $\Gamma\{\mathscr{F}\}$ is the substitution group induced by the isometric substitutions onto the dynamical variables of the rotation internal rotation problem, which may be written as

$$\begin{pmatrix} \alpha' \\ \beta' \\ \gamma' \\ \tau' \\ v_0' \\ v_1' \\ 1 \end{pmatrix} = \Gamma(F) \cdot \begin{pmatrix} \alpha \\ \beta \\ \gamma \\ \tau \\ v_0 \\ v_1 \\ 1 \end{pmatrix} \tag{2-4}$$

where α, β, γ denote the Eulerian angles [15] of the frame system $\tilde{e}^f$ w.r.t. the laboratory system. $\Gamma\{\mathscr{F}\}$ will prove essential in a later paper on the rotation-internal rotation problem of the semirigid ethylene glycol model. If the internal motion Hamiltonian ($J=0$) is expanded to the harmonic approximation in a neighborhood of any r_e structure the harmonic vibrational problem of the corresponding conformation results. Whether the harmonic approximation is sufficient for interpretation of experimental spectra, depends on the behaviour of the electronic energy function in the internal parameter space (2-3), in particular on the energy of the transition points ($r^{\neq}$ structures) between r_e structures (cf. Fig. 2). Strictly speaking the vibrational states of glycol should be discussed within the framework of its complete internal isometric group. From this point of view all states with $J=0$ belong to the irreducible representations of $\mathscr{F}=\mathscr{V}_4$, which however allow identification of particular conformations according to the nuclear configuration density functions given by the eigenfunction of the internal motion problem. The discussion of the infrared spectra given in Section 4 will be made from this point of view.

3. *Ab initio* SCF Calculation

The approximate Hartree-Fock atomic orbitals employed as a basis set for the *ab initio* SCF calculation in this work were the Gaussian lobe function representation obtained by Whitten [16]. The basis set included three contractions of 4, 3 and 3 spherical Gaussians for *s* orbitals and five pairs of Gaussians for each of the three *p* orbitals of the carbon and oxygen respectively. Each hydrogen *s* orbital is represented by five spherical Gaussians [17] scaled by a factor $2^{\frac{1}{2}}$, which has been proved to be adequate for the description of molecular environments. Thus the basis set included 130 Gaussians, 70 of *s* and 60 of *p* type (where a *p* function is represented by a pair of *s* functions) for each calculation. These functions are grouped, in turn, so that a total of 30 linear coefficients were left free to be determined by the SCF procedure. This size of the Gaussian lobe function basis set is approximately equivalent to the double-zeta Slater-type orbital basis set in accuracy. For example, it gives energies of -37.68052 a.u. and -74.79154 a.u. for the ^3P atomic state of carbon and oxygen respectively, while the corresponding energies from the double-zeta Slater-type basis set are -37.68867 a.u. and -74.80418 a.u. [16].

Calculations are carried out employing geometrical parameters determined by the microwave spectra on 2-chloroethanol [8] and methanol [18] which are summarized in Table 3. Figure 1b defines the torsional angles in ethylene glycol. The all-trans conformation with $2\tau = \upsilon_0 = \upsilon_1 = 180°$ is included since in this conformation the distance between the hydrogens in both OH groups is the longest and therefore the effect of the hydrogen bond is considered to be minimal. Table 4 lists the molecular SCF energies of all NC considered in the calculation along with energy differences between these and the energy minimum conformer, $\upsilon_0 = -30°$, $\upsilon_1 = 60°$. In Table 5 the results are contrasted with those of Radom *et al.* [3] for all conformations where common data are available.

Figure 2 represents a level chart of the electronic energy function for constant value $2\tau = 60°$ obtained from 26 calculated points by interpolation in the interval

$$\begin{aligned} -\pi \leqq \upsilon_0 < +\pi \\ -\pi \leqq \upsilon_1 < +\pi \end{aligned} \qquad (2\text{-}3')$$

with the origin shifted to $\upsilon_0 = -120°$, $\upsilon_1 = -120°$. This shift has been chosen to show explicitely the isometric symmetry V_2 $2\tau' = 2\tau = 60°$, $\upsilon_0' = \upsilon_1$, $\upsilon_1' = \upsilon_0$

Table 3. Geometrical parameters adopted for the *ab initio* calculation of ethylene glycol

Bond distances (Å)		Bond angles	
C–C (R_1)	1.519	<CCO (α)	112.77°
C–O (R_2)	1.411	<CCH	111.40°
C–H($\lvert X^F_{FOO}\rvert$)	1.093	<HCH	108.67°
O–H	0.945	<COH	108.53°
O–H'[a]	1.008	<COH'[a]	105.77°

[a] H' stands for the hydrogen in the O–H'–O hydrogen bond.

Table 4. Molecular SCF energies of ethylene glycol

υ_0	υ_1	$\mathscr{E}(2\tau = 60°, \upsilon_0, \upsilon_1)$[a]	$\Delta\mathscr{E}$[b]
0°	0°	−228.6791	4.01
0°	60°	−228.6833	1.38
0°	120°	−228.6780	4.71
0°	180°	−228.6774	5.08
0°	−120°	−228.6744	6.97
− 30°	0°	−228.6768	5.46
− 30°	60°	−228.6855	0.00
− 30°	120°	−228.6821	2.13
− 30°	180°	−228.6821	2.13
− 30°	−120°	−228.6796	3.70
− 60°	30°	−228.6798[d]	3.58
− 60°	60°	−228.6837	1.13
− 60°	90°	−228.6835	1.25
− 60°	120°	−228.6821	2.13
− 60°	150°	−228.6818	2.32
− 60°	180°	−228.6826[d]	1.82
− 60°	−150°	−228.6825	1.88
− 60°	−120°	−228.6825	1.88
− 60°	− 90°	−228.6824	1.95
− 60°	− 60°	−228.6802[d]	3.33
− 90°	60°	−228.6785	4.39
− 90°	120°	−228.6767	5.52.
− 90°	180°	−228.6780	4.71
− 90°	−120°	−228.6795	3.77
30°	30°	−228.6822	2.07
180°	180°	−228.6702[d]	9.60
180°[c]	180°[c]	−228.6743[d]	7.03

[a] Atomic units.
[b] $\Delta\mathscr{E} = \mathscr{E}(60°, \upsilon_0, \upsilon_1) - \min \mathscr{E}(60°, \upsilon_0, \upsilon_1)$, kcal/mol units.
[c] Trans conformation with respect to C–C bond ($2\tau = 180°$).
[d] These points have been calculated in Ref. [3].

Table 5. Comparison of molecular SCF energies[a]

Notation		$\mathscr{E}$ (a.u.)		$\mathscr{E} - \mathscr{E}_{min}$ (kcal/mol)		Difference in SCF energies (kcal/mol)
Ref. [3]	This work	Ref. [3]	This work	Ref. [3]	This work	
	$\upsilon_0 = -30°/\upsilon_1 = 60°$[b]		−228.6855		0.00	
tGg'[c]	$\upsilon_0 = -60°/\upsilon_1 = 180°$	−228.59605	−228.6826	0.00	1.82	54.36
tTt	$\upsilon_0 = 180°/\upsilon_1 = 180°$	−228.59285	−228.6743	2.01	7.03	51.16
gGg'	$\upsilon_0 = -60°/\upsilon_1 = 60°$	−228.59245	−228.6837	2.26	1.13	57.31
tGt	$\upsilon_0 = 180°/\upsilon_1 = 180°$	−228.58698	−228.6702	5.69	9.60	52.29
	$\upsilon_0 = 30°/\upsilon_1 = 30°$		−228.6822		2.07	
gGg	$\upsilon_0 = 60°/\upsilon_1 = 60°$	−228.58648		6.01		
$g'Gg'$	$\upsilon_0 = -60°/\upsilon_1 = -60°$	−228.58792	−228.6802	5.10	3.33	57.94

[a] Only for those conformations where comparisons can be made. Ref. [3]: basis set 4–31 *G*. This work: Whitten's Gaussian lobe extended basis set, see text.
[b] Minimum energy conformation of this work.
[c] Minimum energy conformation of Ref. [3].

(cf. Table 2) of the electronic potential function. The line $\upsilon_0 = \upsilon_1$ corresponds to fixed point NC's [14]. Several interesting features may be derived from Fig. 2 and Table 4, in which numerical values of $\mathscr{E}$ as a function of τ, υ_0, and υ_1 are given.

Before entering discussion, it should be mentioned that only one computation with $2\tau \neq 60°$ has been carried out. It nevertheless is felt that the body of data computed in this work is sufficient for a fairly complete discussion of all relative nuclear configurations relevant for conformations involving internal hydrogen bonding.

1. r_e-structures with lowest minima of $\mathscr{E}$ are assumed for $2\tau = 60°$, i.e. for gauche conformation with respect to the C–C bond. The gauche conformer without internal H-bonds ($\upsilon_0 = \upsilon_1 = \pm 180°$) has 9.60 kcal/mol (40.17 kJ/mol) higher energy than the lowest energy conformation and the all-trans conformer $2\tau = 180°$, $\upsilon_0 = \upsilon_1 = 180°$, has 7.03 kcal/mol (29.41 kJ/mol) higher energy than the latter. The energy difference of 2.03 kcal/mol of these two conformations with no internal H bond may be due to repulsive lone pair interaction of the gauche ($2\tau = 60°$) conformer. The all-trans conformer corresponds to an energy minimum with respect to τ at fixed $\upsilon_0 = \upsilon_1 = 180°$.
2. The r_e structure with lowest energy minimum is found at $2\tau_e = 60°$, $\upsilon_{0e} = -30°$, $\upsilon_{1e} = 60°$ (cf. Table 4) and corresponds to a conformation in which the O–H...O bonded proton is located nearest to the sp^3 lone pair of the acceptor O atom, whereas the shortest distance proton-acceptor O atom is assumed to be at $\upsilon_0 = -28°$. This obviously implies that the Pitzer potential [21] associated with the internal rotation about the C–C bond is dominated by internal H bonding, which forces the proton to a position nearest to the acceptor O atom. On the other hand the value of $\upsilon_{1e} = 60°$ means that one of the lone pair orbitals of the acceptor O atom is directed (in the sense of directed valence [19, 20]) towards the proton involved in the H bond.
3. The 2nd r_e structure with $2\tau_{e2} = 60°$, $\upsilon_{0e2} = -45°$ and $\upsilon_{1e2} = -160°$ corresponds to a conformation in which the internal H bond involves the 2nd lone pair of the acceptor O atom. The energy $\mathscr{E}$ (60°, −45°, −160°) lies 2.13 kcal/mol above that of the r_{e1} structure. Calculation shows that both the nuclear-nuclear repulsion energy in a.u., and the electron-electron repulsion energy of the r_{e2} structure are lower than those of the r_{e1} configuration:

	r_{e1}	r_{e2}
nuclear repulsion	133.2038	132.7007 a.u.
electronic repulsion	215.3096	214.9888 a.u.

However, the difference in nuclear-electron and kinetic energy dominate in determining the relative stability of the two conformers, as is shown by the following values:

	r_{e1}	r_{e2}
nuclear-electron attraction	−806.7298	−805.9041 a.u.
kinetic energy	229.5300	229.5325 a.u.

4. In connection with the isometric group it has been stated in Section 2 that isometric r_e structures always occur in sets of four. Figure 2 shows one pair of each of the r_{e1} and r_{e2} structures, thereby illustrating the nature of the multi-minimum problem determining the conformation problem of glycol. The transition point $r^{\neq}_{1,1}$ between the two r_{e1} structures $2\tau_{e1} = 60°$, $\upsilon_{0e1} = -30°$, $\upsilon_{1e1} = +60°$, and $2\tau_{e1} = 60°$, $\upsilon_{0e1} = +60°$, $\upsilon_{1e1} = -30°$ corresponds to a barrier of $V^{\neq}_{11} \sim 2$ kcal/mol. This numerical value of $V^{\neq}_{11}$ should be considered as rather uncertain and in reality may be higher since no attempt has been made to optimize other important geometrical parameters such as τ, the COH-angle and the OH distances. From Table 2 it can be seen that the two conformations are properly congruent, since the rotative part of $\Gamma^{(NC)}$ is properly orthogonal. Furthermore, transitions between them mainly involves the two C–OH torsional modes (cf. Section 4).
5. Similar discussion may be devoted to the transition point between r_{e1} and r_{e2} conformations with $\upsilon^{\neq}_{0,12} \approx -45°$, $\upsilon^{\neq}_{1,12} \approx 150°$, for which a value of

$$V^{\neq}_{1,2} = \mathscr{E}^{\neq}_{1,2} - \mathscr{E}(r_{e1}) \approx 2 \text{ kcal/mol}$$

is derived. It obviously corresponds to a rather flat plateau type saddle point; again transitions between r_{e1} and r_{e2} conformations would mainly involve the two C–OH torsional modes.
6. It is worthwhile to consider briefly the region $\upsilon_0 \approx \upsilon_1 \approx -75°$ of the electronic potential surface ($2\tau = 60°$), which represents nuclear configurations with two internal H bonds. According to Table 4 and Fig. 2 no local minimum exists in this region but rather a saddle point $r^{\neq}_{2,2}$, which determines the dynamics of transitions between r_{e2} conformations. The barrier height above the r_{e2}-level amounts to approximately 0.8 kcal/mol.

4. Infrared Matrix Spectra and Discussion of Conformations

The matrix data presented in this work indicate at least two different OH torsional states of the gauche C–C conformer with a single internal hydrogen bond. At this stage the interpretation is based on the conformations r_{e1} and r_{e2} (see Fig. 2).

4.1. Experimental

Samples of CH_2OHCH_2OH were purchased from FLUKA AG, Buchs, Switzerland, and samples of CD_2OHCD_2OH from ROTH GMBH, Karlsruhe, Germany. They were used for spectroscopical purposes after drying with MOLECULAR SIEVES A 3. 20 g of the species CH_2ODCH_2OD were prepared in this laboratory by hydrolysis of 15 g of ethylene oxide with 250 ml of D_2O. The spectrum of this sample shows only a trace of an OH stretching absorption indicating an isotopic purity of at least 98%.

The three species were isolated at M/A 3000 in Argon matrices at liquid Helium temperature. The spectra were measured at a resolution of 0.5–3 cm^{-1} with a Perkin-Elmer Model 325 spectrometer. The regions which are of interest for the present work are shown in Figs. 3–5. For the deposition of the matrices,

sample vapour and matrix gas were fed through separate inlets controlled by BROOKS needle values. In order to investigate the effect of different vapour temperatures, the sample vapour was heated, in part of the experiment, to 160° C in a Knudsen cell [22] before depositing onto the cold CsI-window.

4.2. Conformational Effects in Matrix Spectra

The main experimental findings are the following:

1. If the sample vapour is heated to $T_2 = 160°$ C before deposition on the cold window, the spectrum is the same as the one obtained with the sample vapour at room temperature ($T_1 = 25°$ C) before deposition.
2. A number of fundamentals are split into doublets or quartets with splittings up to 30 cm^{-1} for localized modes (see Figs. 3–5).

Three experiments with higher vapour temperature $T_2 = 160°$ C were made in order to populate high temperature conformations such as the *trans* C–C conformer which has no internal hydrogen bond. In such spectra the absorptions due to high energy conformers should be enhanced if relaxation to low energy conformers during the condensation of the matrix may be excluded. With the present choice of the two temperatures the effect should be most pronounced for an energy separation of 200–800 cm^{-1} between those conformers having no internal H bond and the energy minimum conformer r_{e1}. No differences in relative absorption intensities could be detected at the two temperatures T_1 and T_2. Such a result should be expected from the large energy separations of the trans and non-bonded gauche conformers from the most stable one (see Table 4). These two facts led us to the conclusion that the trans and non-bonded gauche conformers are virtually absent in the matrix. A similar result was obtained by Buckley and Giguère [5] and Zubkova *et al.* [6, 7] from the gas phase spectra.

A qualitative interpretation of the observed spectra will be attempted in terms of the r_{e1} and r_{e2} conformers obtained from ab initio SCF calculations. Another possibility giving rise to splittings may be the tunnelling between the two equivalent r_{e1}-conformers or r_{e2}-conformers.

Hydroxyl Stretching Region. The stretching patterns shown in Fig. 3 of the species with two OH or two OD groups are essentially the same. In the case of the OH groups the strong band at 3666 cm^{-1} may be assigned to the non-bonded OH group of the r_{e1}-conformer. The weaker satellite at 3680 cm^{-1} might be an out of phase combination of the two OH stretches in the r_{e2}-conformer. The two weakest absorptions in the quartet between 3634 and 3617 cm^{-1} could be due to the bonded OH group either of the r_{e1}-conformer or of the r_{e2}-conformer, split by about 12 cm^{-1}, owing to the tunnelling. Similarly, the two stronger absorptions in the quartet would then arise from the r_{e1}- or the r_{e2}-conformer, respectively.

CH_2 *Scissoring and Wagging Region.* The relatively strong and sharp band at 1495 cm^{-1} (see Fig. 4) can be attributed with fair confidence to the CH_2 bending mode next to the non-bonded OD group in the r_{e2}-conformer of the species OD–CH_2–CH_2–OD. This result was found in the preliminary normal coordinate analysis (NCA). The set of three weaker bands between 1470 and 1460 cm^{-1} contains the bending mode of the CH_2 group next to the bonded OD

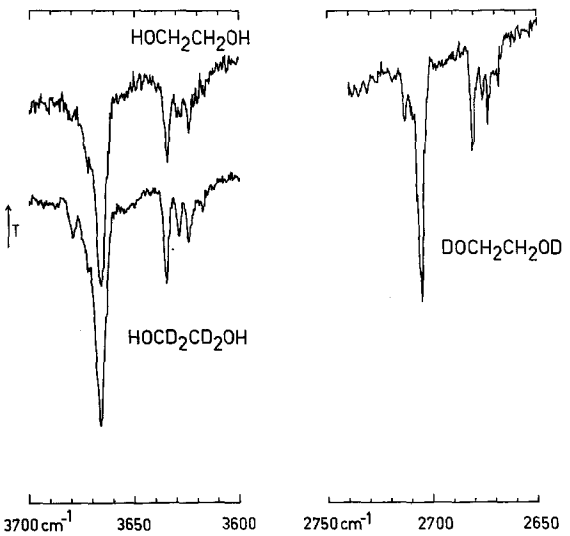

Fig. 3. Ar-matrix spectra at M/A ~ 3000 in the OH and OD-stretching regions

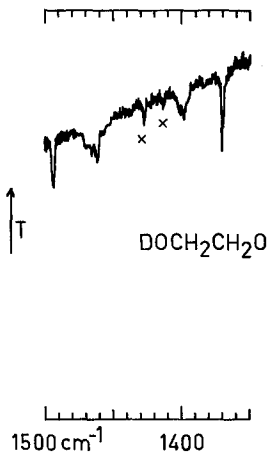

Fig. 4. Ar-matrix spectrum at M/A ~ 3000 in the CH_2-scissoring and wagging region of $DOCH_2CH_2OD$. The absorptions marked with x are due to the HOD-impurity

group of the r_{e2}-conformer as well as in phase and out of phase combinations of the CH_2 bendings in the r_{e1}-conformer. The shift of this group of three frequencies from the one at 1495 cm^{-1} was reproduced within a few wave numbers by the NCA and is mainly due to a *G*-matrix effect.

No conformational effects were found for the CH_2 wagging modes (see Fig. 4). The broad band at 1402 cm^{-1} is assigned to the wagging mode of the CH_2 group next to the non-bonded OD group of both r_{e1}- and r_{e2}-conformers while the sharper feature at 1370 cm^{-1} arises from the CH_2 group next to the bonded

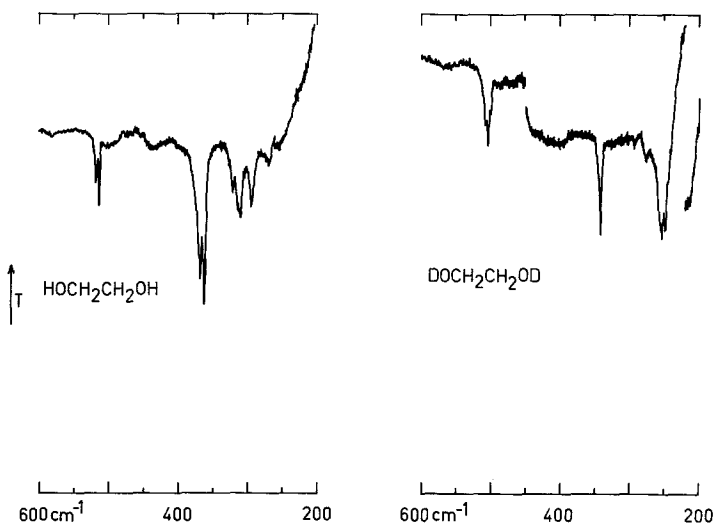

Fig. 5. Ar-matrix spectra at M/A ~ 3000 showing the skeletal bending, OH-torsional and higher OD-torsional absorptions

OD group, again of both r_{e1}- and r_{e2}-conformers, according to the NCA. The calculated spacing between the two wagging modes of a given conformer was about 32 cm^{-1}, in accordance with the observed frequencies.

Skeletal Bending and OH *Torsional Region.* The out of phase combination of the CCO bendings is found as a doublet near 516 cm^{-1} for the parent species and as a less resolved triplet centered at 504 cm^{-1} for the species CH_2ODCH_2OD. The corresponding in phase bending modes are at 315 and 342 cm^{-1}, respectively (see Fig. 5). The torsions of the bonded OH and OD groups are located near to 364 and 252 cm^{-1}, respectively, while the torsion of the non-bonded OH group occurs at 281 cm^{-1}. A clear doublet structure is observed for the hydroxyl torsions, and in the case of the parent species for the skeletal bendings. This might be due to splittings between r_{e1}- and r_{e2}-conformers, since similar splittings between the two conformers are obtained from the NCA. However, double minimum tunnelling should also be considered as a possible explanation for these splittings.

The OH torsional force constants used to reproduce the observed frequencies are 0.066 and 0.036 mdyn/rad for the bonded and the non-bonded OH group, respectively. In our preliminary NCA the two torsions are almost uncoupled. The potential well for the r_{e1}-conformer, as obtained from the calculated energy surface (see Fig. 2) indicates, however, a strong coupling in the potential energy of the two torsions. According to this, the two torsional modes should be in phase and out of phase combinations rather than individual torsions of the two OH groups. The respective force constants estimated from the calculated energy surface agree within only about 10% with the values used in the NCA, if these are associated with the in phase (0.036 mdyn/rad) and out of phase (0.066 mdyn/rad) combinations. With this modification, there seems to be a good agreement

between the calculated potential well and the experimental data. On the other hand, if the OH torsional modes of the r_{e2}-conformer are indeed close to those of the r_{e1}-conformer, the respective force constants should be approximately equal. This, however, is in contradiction with the obvious shallowness of the calculated potential function for the r_{e2}-conformer (see Fig. 2).

For the r_{e1}-conformers, the zero point energy is about 330 cm^{-1}. That is, the zero point energy is about 400 cm^{-1} below the saddle point between the two equivalent r_{e1}-conformers of the potential surface. This means that the double minimum tunnelling might be significant. A more quantitative analysis of these effects is in progress.

5. Conclusion

The experimental data confirm the results from the calculation in so far as only gauche C–C conformers of ethylene glycol with a single internal hydrogen bond have been detected experimentally at room temperature. The potential function calculated for the r_{e1}-conformer seems to be in fair agreement with the present experimental data. The calculated potential function of the r_{e2}-conformer, however, may be too high in energy and too shallow. This indicates possible shortcomings either of the calculation or of the experimental situation. A refinement of the calculation by allowing for the relaxation of the C–C torsional angle or other geometrical parameters may well produce a more accurate picture of the relative height and of the shapes of the two non-equivalent potential wells. On the other hand, as far as the experiment is concerned, it is not known to what extent the Ar-matrix affects the relative stability of the two conformations. It should be mentioned at this point that irradiation by infrared induces irreversible changes of the matrix spectra which are not yet fully understood. For analysis of this phenomenon, which clearly indicates the existence of relaxation processes of the matrix isolated glycol molecule, further experiments are designed. Such a study should yield a key to a reliable assignment of the spectra to particular conformations of the glycol molecule isolated in a rare gas matrix. They furthermore should allow discrimination between multiple minima transitions and the presence of different conformers even at LHe temperature.

Acknowledgement. We wish to express our gratitude to the Swiss National Foundation (Project Nr. 2.606.72 and Nr. 2.808.73) and to Messrs. Sandoz AG., Basel, for financial support. The ETH-Z Computation Center granted generous computer time and valuable technical assistance by Mrs. A. Günter and Mr. P. Nyffeler is acknowledged.

References

1. Pachler, K.G.R., Wessels, P.L.: J. Mol. Struct. **6**, 471 (1970)
2. Matsuura, H., Hiraishi, M., Miyazawa, T.: Spectrochim. Acta **28** A, 2299 (1972)
3. Radom, L., Lathan, W.A., Hehre, W.J., Pople, J.A.: J. Am. Chem. Soc. **95**, 693 (1973)
4. Bastiansen, O.: Acta Chem. Scand. **3**, 415 (1949)
5. Buckley, P., Giguere, P.A.: Can. J. Chem. **45**, 397 (1967)
6. Zubkova, O.B., Shabadash, A.N.: Zh. Prikl. Spektr. **14**, 874 (1971)
7. Zubkova, O.B., Gribov, L.A., Shabadash, A.N.: Zh. Prikl. Spektr. **16**(2), 306 (1972)

8. Azrak, R. G., Wilson, E. B.: J. Chem. Phys. **52**, 5652 (1970)
9. Buckton, K. S., Azrak, R. G.: J. Chem. Phys. **52**, 5299 (1970)
10. Penn, R. E., Curl Jr., R. F.: J. Chem. Phys. **55**, 651 (1971)
11. Busfield, W. K., Ennis, M. P., McEwen, I. J.: Spectrochim. Acta **29** A, 1259 (1973)
12. Podo, F., Némethy, G., Indovina, P. L., Radics, L., Viti, V.: Mol. Phys. **27**, 521 (1974)
13. Scott, R. A., Scheraga, H. A.: J. Chem. Phys. **45**, 2091 (1966)
14. Bauder, A., Meyer, R., Günthard, Hs. H.: Mol. Phys., in press. The reader should consult this paper for detailed discussion and relations to the Longuet-Higgins group of non-rigid molecules
15. Edmonds, A. R.: Angular momentum in quantum mechanics, p. 7. Princeton: University Press 1957
16. Whitten, J. L.: J. Chem. Phys. **44**, 359 (1966)
17. Whitten, J. L.: J. Chem. Phys. **39**, 349 (1963)
18. Lees, R. M., Baker, J. G.: J. Chem. Phys. **48**, 5299 (1968)
19. Eyring, H., Walter, J., Kimball, G. E.: Quantum chemistry, p. 227. London: Wiley 1947
20. Hartmann, H.: Theorie der Chemischen Bindung auf Quantentheoretischer Grundlage, p. 164. Berlin-Göttingen-Heidelberg: Springer 1954
21. Pitzer, K. S.: Discussions Faraday Soc. **10**, 66 (1951)
22. Frey, R.: Thesis, ETH-Zürich 1969
23. Ditchfield, D., Hehre, W. J., Pople, J. A.: J. Chem. Phys. **54**, 724 (1971)

Dr. T.-K. Ha
Eidgenössische Technische Hochschule
Laboratorium für Physikalische Chemie
CH-8006 Zürich
Universitätsstraße 22, Switzerland